# Supplementary information

## Eco-friendly biogenic hydrogel for wearable skin-like iontronics

Huawen Liu [a], Donghua Xu [b], Bin Hu [c], Junjie Jiang [d], Mengya Li [a], Dan Zhao [a], Wentao Zhai *[a]

[a] *School of Materials Science and Engineering, Sun Yat-sen University, Guangzhou, Guangdong, 510275, China*

[b] *State Key Laboratory of Polymer Physics and Chemistry, Changchun Institute of Applied Chemistry, Chinese Academy of Sciences, Changchun, Jilin, 130022, China*

[c] *College of Science, China University of Petroleum (Beijing), Beijing, 102249, China*

[d] *Ningbo Institute of Materials Technology and Engineering, Chinese Academy of Sciences, Ningbo, Zhejiang, 315201, China*

*Corresponding Author: W. Zhai (E-mail: zhaiwt3@mail.sysu.edu.cn)*

**This material includes**

**Experimental Section**

**Supplementary Figures**



**Supplementary Movies**

two VHB tapes.

**Movie S3** The 3D printing characteristics of cassava hydrogel.

**Movie S4** Response time of skin-like capacitive iontronics.

**Movie S5** Response time of skin-like resistive iontronics.

**Movie S6** Capacitance change of capacitive iontronics as the finger was bent optionally.

**Movie S7** Resistance change of resistive iontronics when the finger was bent optionally.

**Movie S8** Resistive iontronics were used to detect facial micro-expression.

**Movie S9** Resistance change when the resistive iontronics were touched slightly.

**Movie S10** The rapid healing process of two fractured cassava hydrogel.

## Experimental Section

***Materials***: Cassava starch was dried for further use. Rhodamine B (RB) and methylene blue (MB) were purchased from Aladdin Chemical Co. Deionized water was used to prepare cassava hydrogel.

***Preparation of Cassava Hydrogel***: Cassava hydrogel was obtained by mixing cassava starch and deionized water in a ratio of 3:7, and then mechanically stirring at 90 $^{o}$C for 1 h. To completely remove air bubbles, the as-prepared cassava hydrogel was deaerated in a vacuum-rotary deaerator (SMIDA, TMV-310T, Shenzhen) for 3 min. The vacuum degree was 10 kPa and the centrifugal speed was 2000 rpm. What is more, the dyed RB/hydrogel and MB/hydrogel were prepared by adding 0.06 wt.% rhodamine B and 0.48 wt.% methylene blue in cassava hydrogel before heating, respectively. In particular, the content of cassava in the 3D-printed hydrogel was 40 wt.%.

***Fabrication of Capacitive Strain and Pressure iontronics***: A dielectric double-sided VHB tape (3M, 4910, with a thickness of 1 mm) was sandwiched between two layers of the stretchable cassava hydrogel, which were then connected by two metal wires, resulting in a capacitive strain and pressure iontronics. Unless otherwise stated, excess two layers of VHB tapes were wrapped around the top and bottom of the device to prevent evaporation of water and insulate the iontronics.

***Fabrication of Resistive Strain and Pressure iontronics***: Two dielectric VHB layers were coated on both sides of the stretchable cassava hydrogel. The both ends of the cassava hydrogel were connected by two metal wires to form a resistive strain and pressure iontronics.

***3D Printing of Cassava Hydrogel***: 3D-printed iontronics were manufactured by printing cassava hydrogel through a 3D printing system (Bio-Architect®-Pro, Regenovo). The 3D-printed models were pre-modeled in the supporting software. The inner diameter of the needle was 0.26 mm. Extrusion pressure was 0.5 MPa and the extrusion speed was 1 mm $s^{-1}$. During the printing process, cassava hydrogel underwent shear-thinning behavior during extrusion, and then quickly returned to its original high viscosity state after extrusion, which allowed for shape maintenance. The entire printing process of cassava hydrogel was kept at room temperature.

***Fabrication of 3D-printed iontronics***: The structure of 3D-printed iontronics was similar to the capacitive strain and pressure iontronics, except that one of the hydrogel components was replaced by a 3D-printed RB/hydrogel. The dyed RB/hydrogel was pre-printed on a double-sided VHB tape and then assembled into a 3D-printed iontronics.

***Characterization***: The morphology and microstructures of the cassava starch and cassava hydrogel were observed by scanning electron microscopy (SEM, EM-30AX, COXEM). Fourier transform infrared (FTIR, Nicolet 6700) was used to characterize the molecular structure of cassava. Raman spectra were characterized by using a micro-Raman spectrometer (inVia Qontor, RENISHAW) in the 632 nm laser excitation with 16.5 mW × 10% power. X-ray diffraction (XRD, PANalytical, Empyrean) was used to characterize the crystallization of cassava starch and cassava hydrogel. All of the above characteristics were performed by using freeze-dried cassava hydrogel. The light transmittance of cassava hydrogel was characterized by UV-visible near infrared spectrophotometer light analyzer (UV-Vis-NIR, UV-3600, Shimadzu). Electrochemical workstation (CHENHUA, CHI660E) was used to investigate the impedance of the hydrogel. The self-healing process of the hydrogel was observed on an optical microscope camera (UOP0500CC) with magnification of 40. The rheological behavior of the cassava hydrogel was tested by using an AR2000ex rheometer (TA Instruments) with 25 mm parallel plate geometry. For rheological measurement of the hydrogel, paraffin oil was applied at the edge of the cassava hydrogel to prevent water evaporation. Steady shear viscosity measurement was investigated within the shear rate range of about $10^{-3}$–$10^{3}$ $s^{-1}$ at 25 °C. Dynamic oscillatory frequency sweep was carried out at 25 °C from 0.1 to 100 Hz in the oscillation mode with the appropriate oscillatory strain of 0.1% within the linear region. Temperature sweep of the hydrogel was tested with the temperature range of 10–50 °C at 0.1% oscillatory strain while the scanning frequency was 1 Hz. Strain sweep measurement was tested within the strain range of 0.01%–2000% at the scanning frequency of 1 Hz at 25 °C. Continuous step-strain sweep was subject to 0.1% strain in the linear regime for 2 min, then back to 200% strain in the nonlinear regime for 1 min, and this process was repeated for several times

at the scanning frequency of 1 Hz. Tensile test and compression test of capacitive and resistive iontronics were performed on a materials testing machine (ETM104, WANCE) at a deformation rate of 25 mm $min^{-1}$ and 0.5 mm $min^{-1}$, respectively. LCR meter (TH2830) was used to detect simultaneous capacitance and resistance changes under various tensile strain and pressures on the device. The capacitance measurements was obtained at a sweeping frequency of 2 kHz and an AC voltage of 5 V. The resistance measurements was obtained at a sweeping frequency of 1 kHz and an AC voltage of 1 V. Volunteer has signed informed consent for the human experiments in this study.

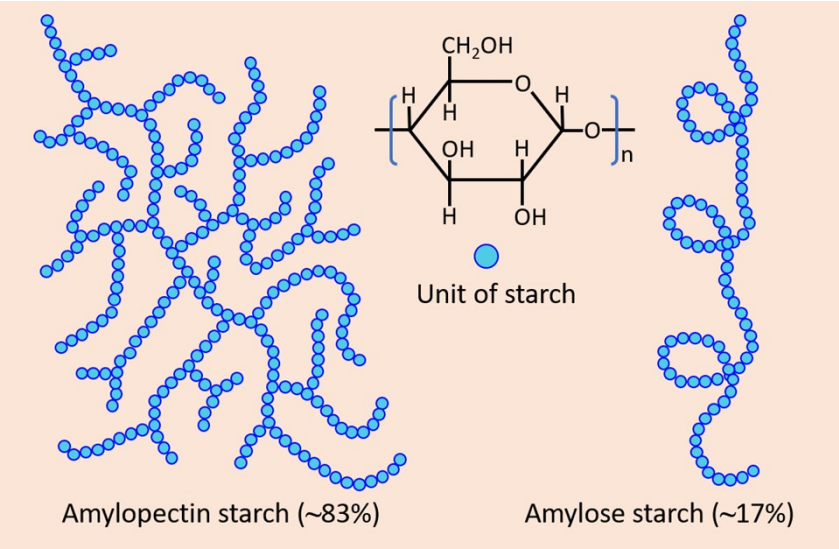


**Fig. S1** The molecular structure of cassava starch. Cassava starch is composed of 83% amylopectin starch and 17% amylose starch.

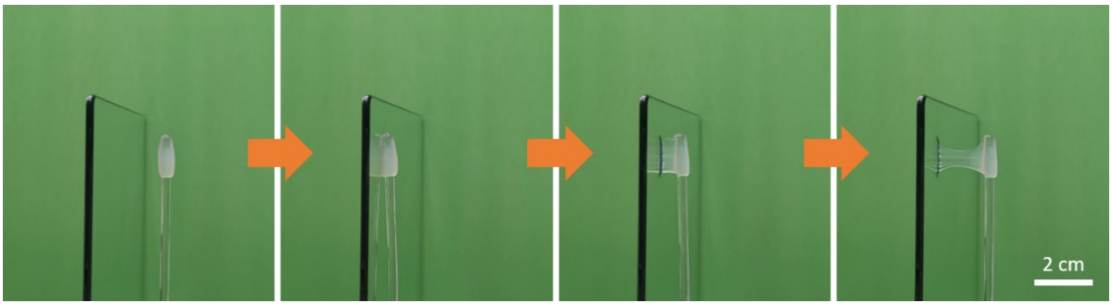


**Fig. S2** The viscosity of cassava hydrogel. The adhesion process of cassava hydrogel and a glass plate.

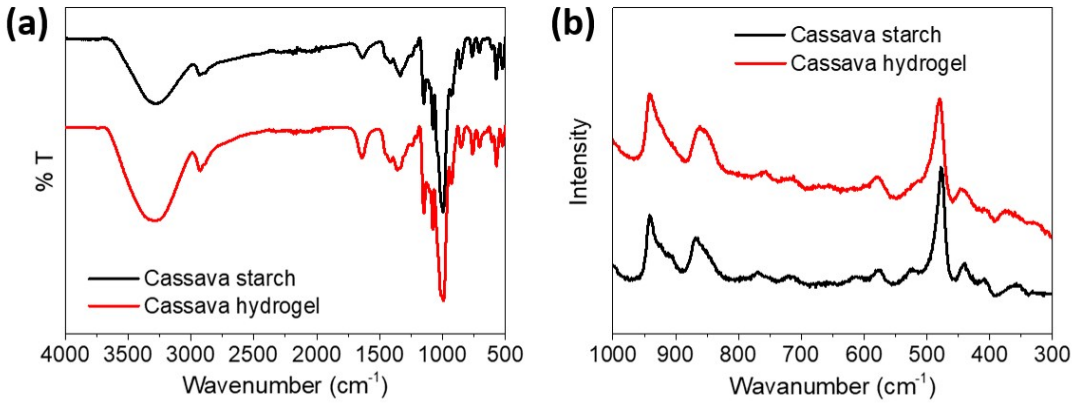


**Fig. S3** (a) Infrared spectra of cassava starch and freeze-dried cassava hydrogel. (b) Raman spectra of cassava starch and freeze-dried cassava hydrogel.

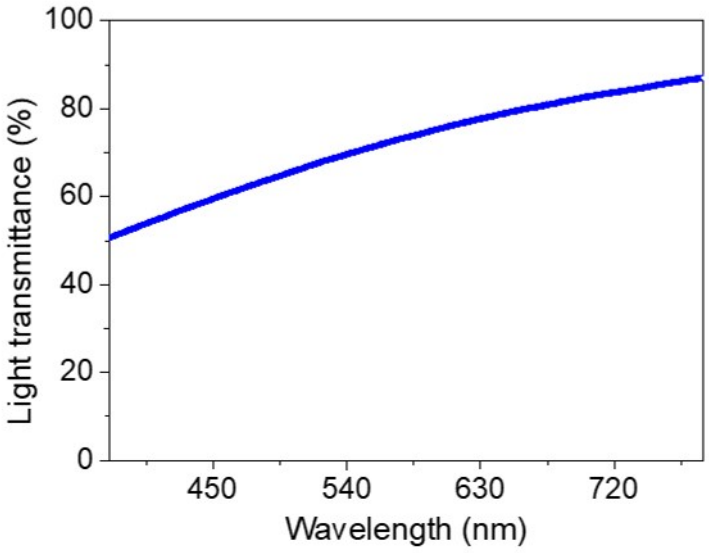


**Fig. S4** The light transmittance of the cassava hydrogel in the visible wavelength range of 380-780 nm. The thickness of the tested sample was 9.5 mm.

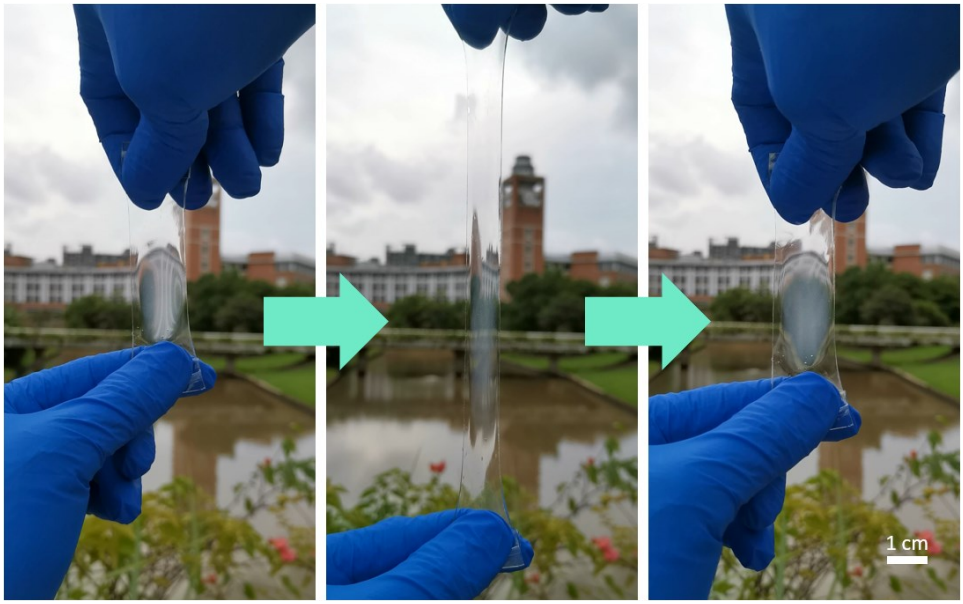


**Fig. S5** Stretching and shrinking process of cassava hydrogel sandwiched between two VHB tapes. The photos are from Movie S2.

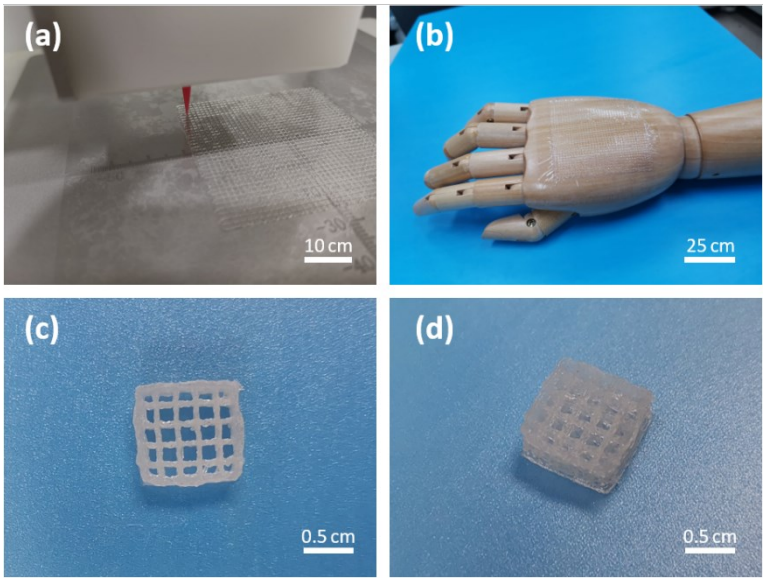


**Fig. S6** (a) Digital photo of the 3D-printed cassava hydrogel. (b) A photo of the 3D-printed iontronics attached to a robotic hand. (c) and (d) Top view and oblique view of 3D-printed cassava hydrogels, respectively.

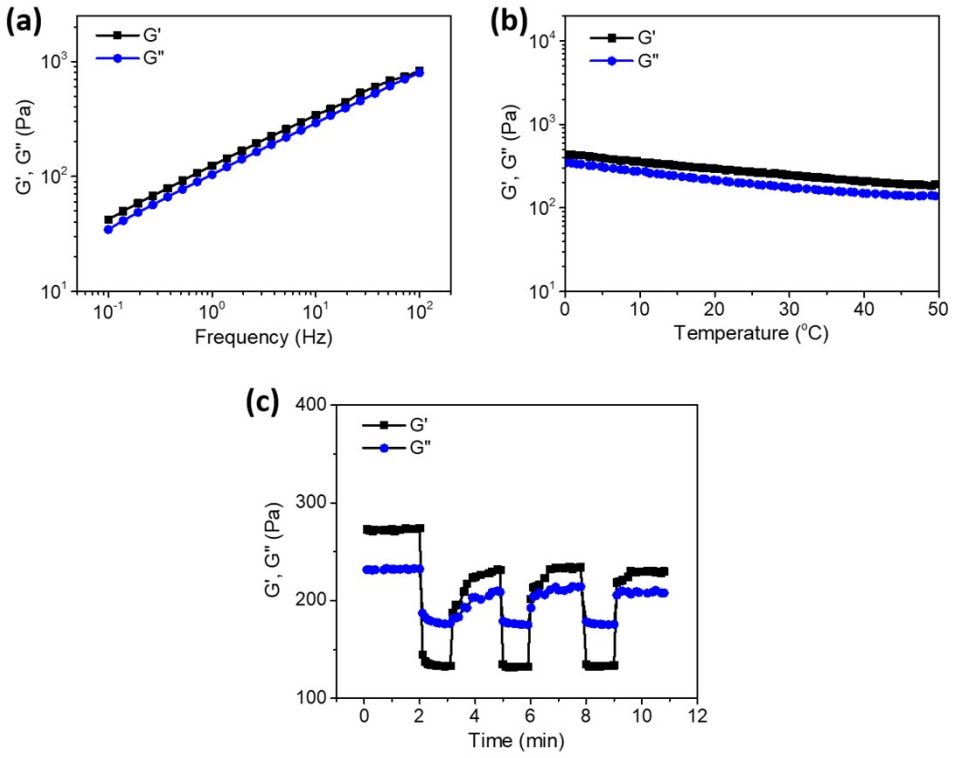


**Fig. S7** (a) Storage modulus ($G'$) and loss modulus ($G''$) versus frequency for the hydrogels. $T$ = 25 °C. (b) $G'$ and $G''$ versus temperature for the hydrogels. Scanning frequency was 1 Hz. (c) $G'$ and $G''$ values of the cassava hydrogel in continuous step strain measurements. The hydrogel was subject to 0.1% strain in the linear strain regime for 2 min, then back to 200% strain in the nonlinear strain regime for 1 min, and this process was repeated for several times, while the scanning frequency was 1 Hz.

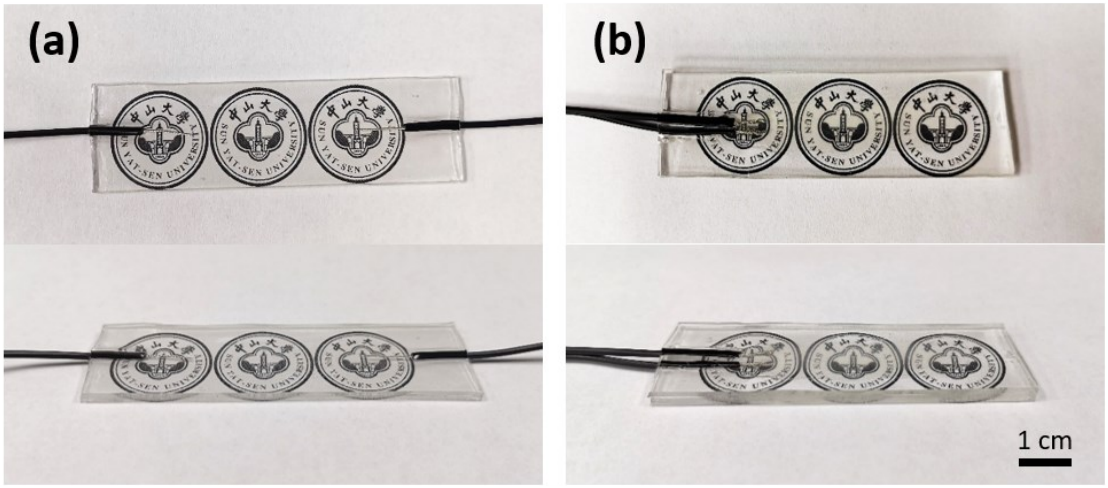


**Fig. S8** Digital photos of hydrogel-based (a) resistive iontronics and (b) capacitive iontronics with dielectric VHB tapes protection, respectively.

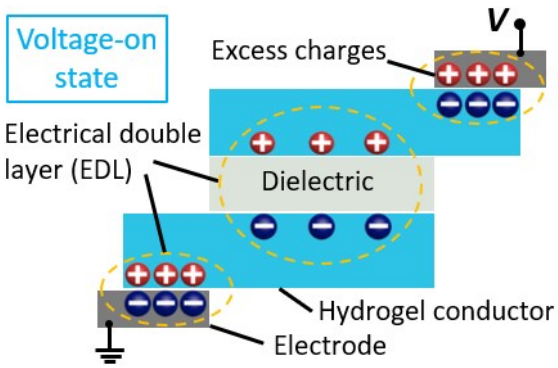


**Fig. S9** The charge distribution of the iontronics in voltage-on state. When a voltage is applied between the two electrodes, the interfaces accumulate additional electric charges. Electrical double layers form at the interfaces between the metal electrodes and the ionic conductive layers, as well as at the interfaces between the ionic conductive layers and the dielectric layers.

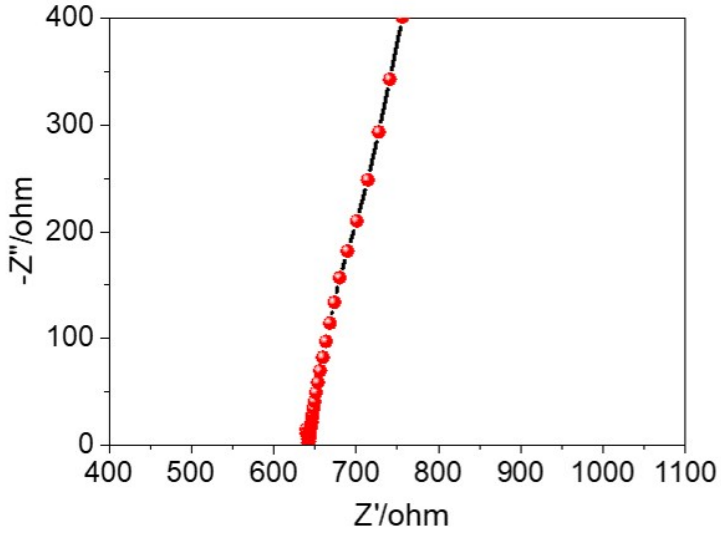


**Fig. S10** Electrochemical impedance spectroscopy of cassava hydrogel. The hydrogel is cylindrical with a thickness of 0.105 cm and a diameter of 1.5 cm. After calculation, The electrical conductivity of the hydrogel is $9.26\times10^{-3}$ S $m^{-1}$.

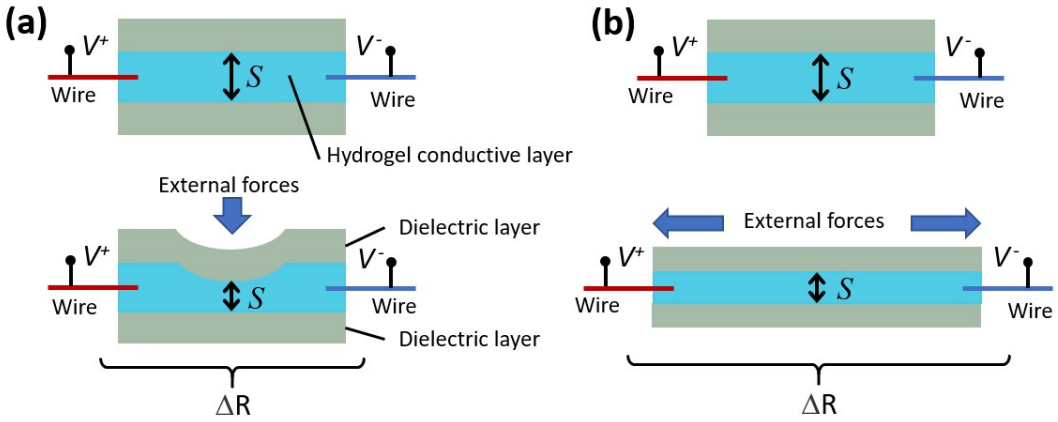


**Fig. S11** The working mechanism of hydrogel-based resistive iontronics. The deformation of the iontronics is based on (a) compression and (b) tension, respectively.

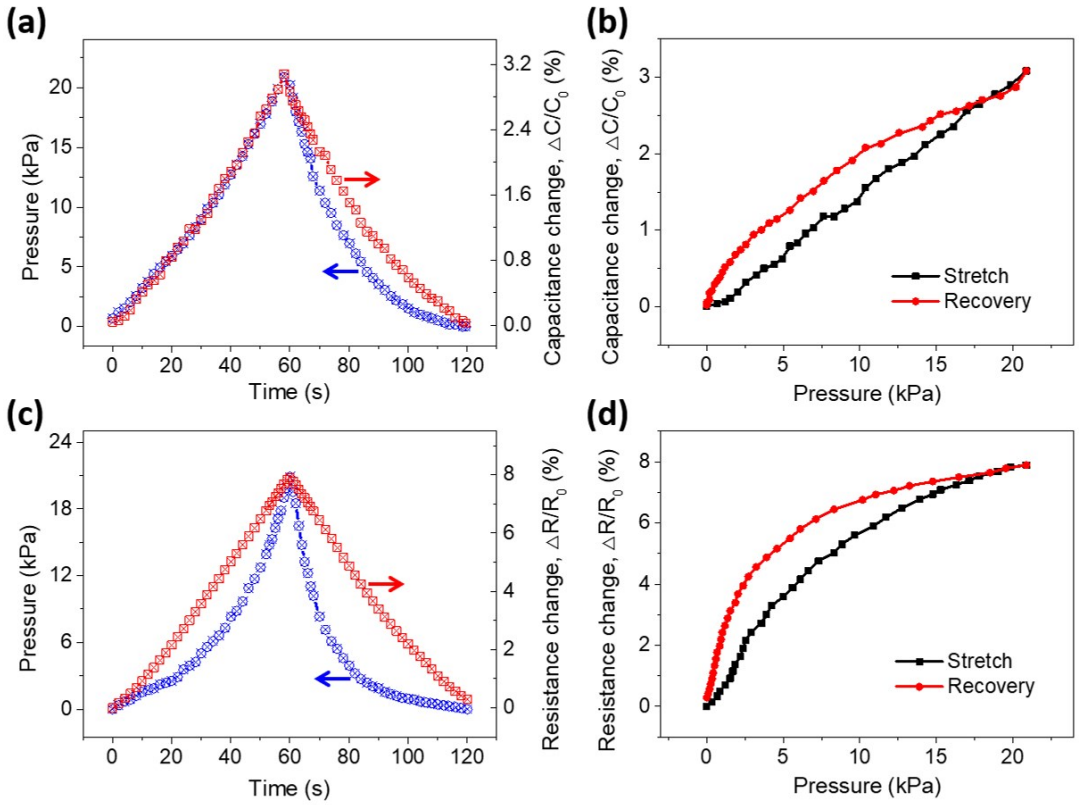


**Fig. S12** (a) The pressure and capacitance of the capacitive iontronics. (b) Pressure–capacitance change curves. (c) The pressure and resistance of the resistive iontronics. (d) Pressure–resistance change curves.

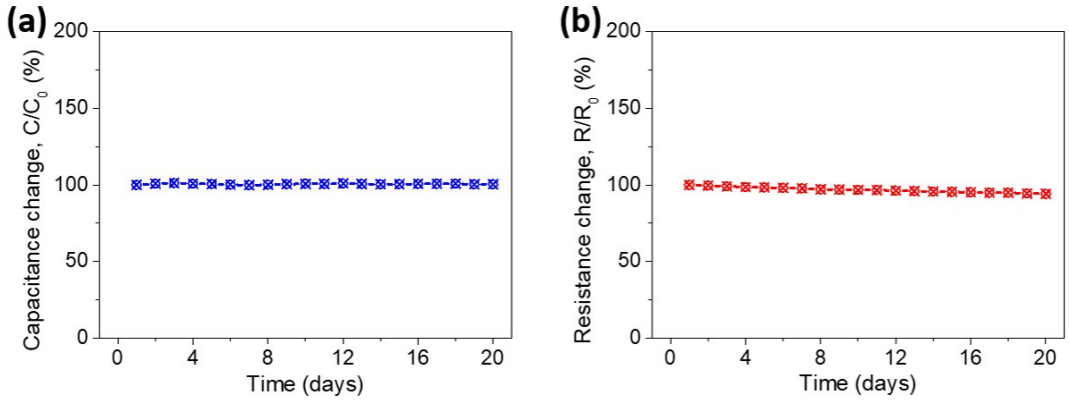


**Fig. S13** Stability of the hydrogel-based iontronics protected by VHB tapes. (a) The capacitance change of capacitive iontronics. (b) The resistance change of the resistive iontronics.

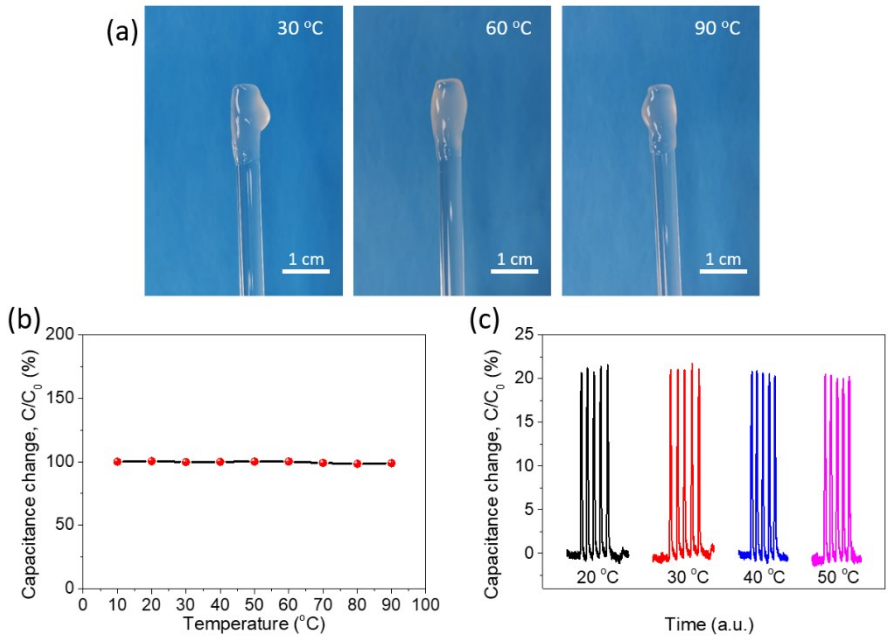


**Fig. S14** The stability of cassava hydrogel and iontronics under different temperature. (a) The digital photos of cassava hydrogel after undergoing different temperatures for 24 h. The cassava hydrogel was sealed in a bottle to test its temperature stability. (b) Capacitances of hydrogel-based capacitive iontronics at different temperatures. (c) The bending-capacitance changes of hydrogel-based capacitive iontronics at different temperatures. The iontronics were attached to the model hands and then placed in an oven at 20 °C, 30 °C, 40 °C and 50 °C. After the temperature was constant, real-time resistance changes of the iontronics when finger bended at 90° was investigated.

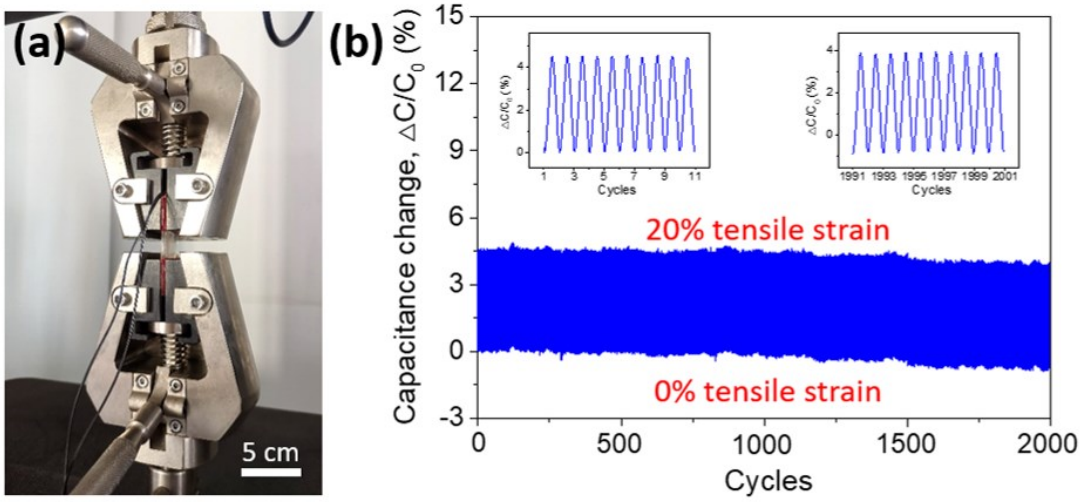


**Fig. S15** Stretching stability of the hydrogel-based iontronics. (a) The capacitive iontronics were placed on the stage of a mechanical testing machine. (b) The tensile strain and capacitance change of the capacitive iontronics cyclically stretched within the strain range of 0-20%, at a frequency of 0.42 Hz.

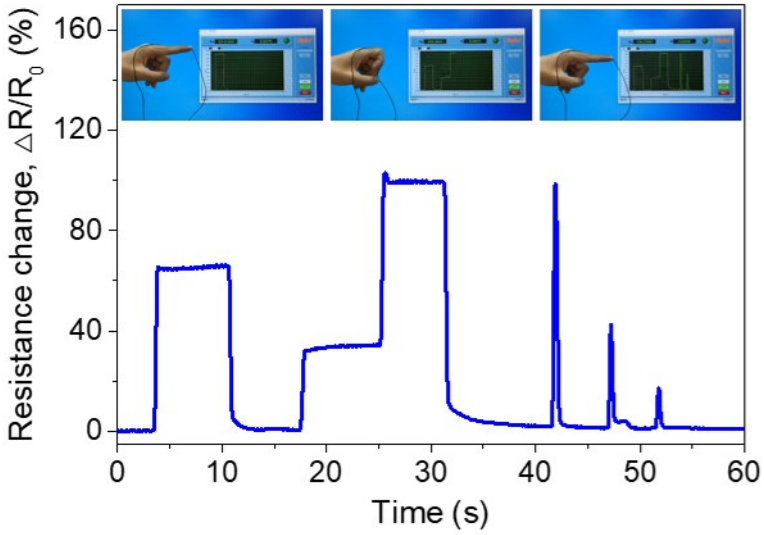


**Fig. S16** Real-time resistance changes when finger bended at different angles. The inset photos are from Movie S7.

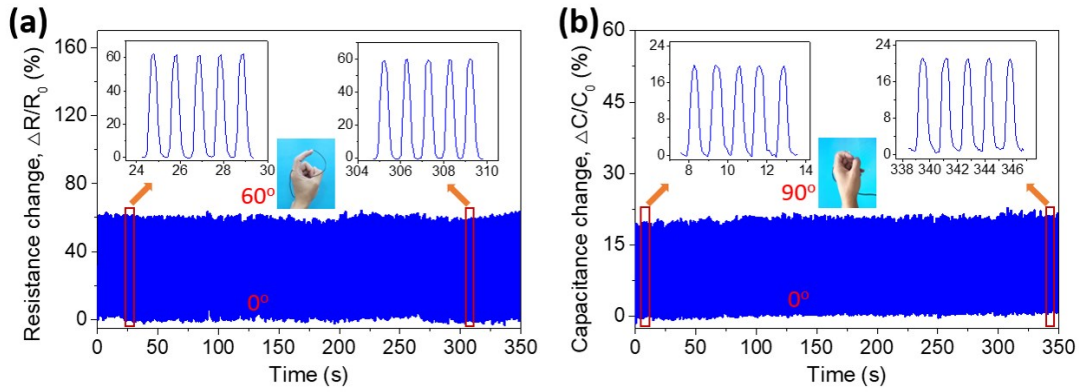


**Fig. S17** Bending stability of the hydrogel-based resistive iontronics. (a) Time and resistance changes of the iontronics cyclically bended up to an angle of 60°. (b) Time and capacitance changes of the iontronics cyclically bended up to an angle of 90°.

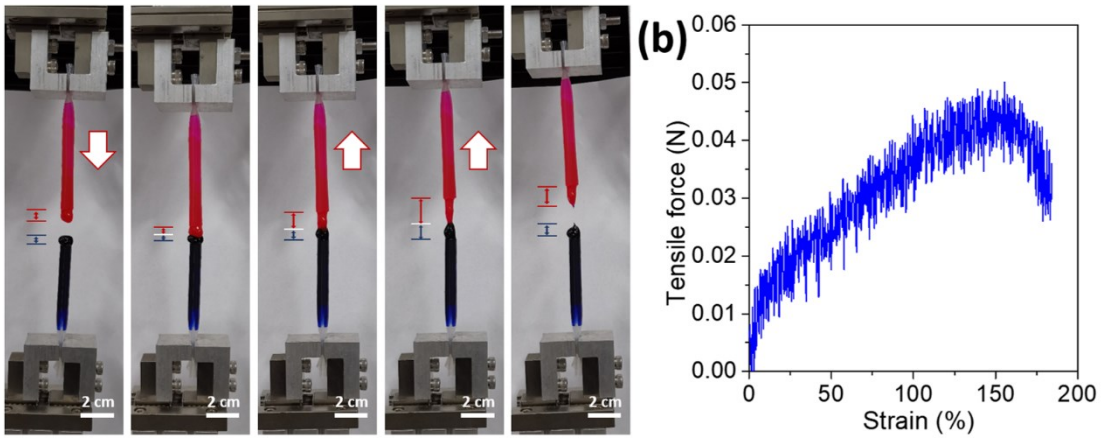


**Fig. S18** Mechanical properties of self-healing hydrogel. (a) Stretching behavior of self-healing cassava hydrogel. Two kinds of cassava hydrogels were dyed by two dyes (rhodamine B and methylene blue), respectively, and then packed in a plastic tube with an exposed length of ~6 mm at one end. After the two hydrogels touched for 10 s, mechanical property of self-healing hydrogel was carried out through a universal testing machine (Lixian Inc.) with an initial length of 12 mm at a stretching speed of 20 mm $min^{-1}$. (b) Strain-force curve of two self-healing hydrogels.